# Swimming and Crawling with an Amphibious Snake Robot

Alessandro Crespi, André Badertscher, André Guignard, and Auke Jan Ijspeert
*Ecole Polytechnique Fédérale de Lausanne (EPFL)*
*School of Computer and Communication Sciences*
*CH-1015 Lausanne, Switzerland*
{*alessandro.crespi,auke.ijspeert*}*@epfl.ch*

***Abstract*— We present *AmphiBot I*, an amphibious snake robot capable of crawling and swimming. Experiments have been carried out to characterize how the speed of locomotion depends on the frequencies, amplitudes, and phase lags of undulatory gaits, both in water and on ground. Using this characterization, we can identify the fastest gaits for a given medium.**

**Results show that the fastest gaits are different from one medium to the other, with larger optimal regions in parameter space for the crawling gaits. Swimming gaits are faster than crawling gaits for the same frequencies. For both media, the fastest locomotion is obtained with total phase lags that are smaller than one. These results are compared with data from fishes and from amphibian snakes.**

***Index Terms*— amphibious robot, snake robot, locomotion characterization, swimming, crawling.**

## I. Introduction

The aim of this project is to build a biologically inspired amphibious snake-like robot, called *AmphiBot I*. The goals of the project are three-fold: (1) to build an amphibious robot for outdoor robotics tasks, taking inspiration from snakes and elongate fishes such as lampreys, (2) to use the robot as a test-bed for novel types of adaptive controllers based on the concept of central pattern generators [1], and (3) to use the robot to investigate hypotheses of how locomotion-controlling neural networks are implemented in real animals.

Such a robot can have multiple applications. On one hand, as mentioned before, it can be used to test neurobiological hypotheses about the structure of the neural networks controlling locomotion in fishes and snakes. On the other hand, the form of an amphibious snake-like robot, its locomotion capabilities and its ability to deal with multiple kinds of environments (including difficult ones) make it well-suited for inspection and exploration tasks (e.g. in areas not easily accessible by humans, such as pipes), and for the participation to *search and rescue* missions (e.g. under a collapsed building or in a flooded zone).

In [15], we presented the robot and the characterization of its crawling. In this article, we carefully characterize the undulatory locomotion of the robot in water and compare it with the crawling. In particular, we investigate how key features of the undulations, namely their frequency, amplitude and phase lag, affect the speed of locomotion in both media. This is important in order to identify which undulations lead to the fastest locomotion for a given environment. It also reveals some interesting differences between the effects of external forces due to friction and to hydrodynamic forces. To the best of our knowledge such a characterization has never been done before for an amphibious snake robot.

We first present some related works (section II), then briefly describe the robot (section III) and the experiments that have been done (section IV). Results are presented in section V, and then discussed in section VI. Finally, propositions for future developments are presented in section VII.

## II. Related works

Snake-like robots are not a recent invention: Hirose and colleagues built in 1972 a robot that is probably the first snake robot [2], generically naming it an *active cord mechanism* (ACM). Some other snake robots have been built by the same group [3]. A very big snake robot has been developed at Caltech in 1992 [4]. In 1994 the NASA Jet Propulsion Laboratory presented a serpentine robot [5]. Miller developed several snake robots prototypes; the last one, named S5 [6], has a very realistic locomotion. In 2002 Saito and colleagues presented a simple snake robot they used to validate theoretical results [7]. In 2003, Conradt developed WormBot [8], a snake-like robot controlled by local CPGs. For a more detailed review of snake robots (including those with powered wheels, not considered here), see [9] and [10].

Swimming snake robots (also referred to as eel or lamprey robots) are less common. There are several theoretical papers about this kind of robots, however there are only few real swimming snake robots. The most interesting robots in this category are *REEL II*, an eel robot [11], the lamprey robot built at Northeastern University [12] and the HELIX-I [13], [14], which uses a particular kind of locomotion derived from the spirochete. In principle, these kinds of robots can be adapted to terrestrial locomotion, but no detailed experiments thereof have been reported.

## III. Description of the hardware

### A. Overview

The robot (visible in Figure 1) has been designed to be modular. It is composed of an adjustable number of identical segments (called *elements*). In this article, we worked with a 7-element robot. The main characteristics of the elements are the following:

- *Waterproofness*: each element is waterproof (as opposed to have a coating of the complete robot), so

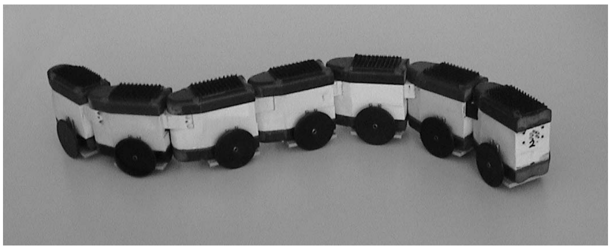

Fig. 1. The complete robot with passive wheels.

that if there is a leakage, only the concerned element is affected and not the whole robot.

- *Independency*: each element has its own power source (battery), motor, and local motor controller.
- *Buoyancy*: the density of an element is close to that of water. Currently it is slightly higher, but we are making small modifications to make it slightly lower than the density of the water, allowing the robot to swim under the water's surface and not to sink in case of failure.
- *Vertical stability*: the center of mass of an element is slightly under the vertical center, so that the robot keeps a stable vertical orientation in water and avoids acquiring a constant angular velocity, which would produce an helicoidal motion.
- *Differential friction coefficients* on the ground: to move using serpentine locomotion, the robot needs to have a lower friction coefficient in the longitudinal axis compared to the perpendicular one. This is achieved with passive wheels in this article.

This kind of design has many advantages, particularly in terms of reliability, scalability and fault tolerance.

### B. Mechanical description

Each element is composed of four main pieces, moulded in polyurethane lightened with phenol microballs: the main body, the top cover, the bottom cover (which contains the battery), and the connection piece. An element has a length of 7 cm and a section of 5.5 (height) by 3.3 (width) cm, including the covers and the connection piece. To ensure the waterproofness, an O-ring is placed between each cover and the body.

The motor drives a set of reduction gears, located in the bottom part of the body, which has a reduction factor of approximately 400. The last gear constitutes the output axis of an element and contains the wires needed to create an electrical connection between the elements (see section III-C). An O-ring ensures the waterproofness of the output axis. Fixed to the output axis is a piece providing electrical and mechanical connections to the next element.

The motor has an integrated magnetic incremental encoder generating 16 pulses per turn, thus allowing a precise determination of the position of the output axis. A potentiometer fixed to the output axis provides an absolute position reference that can be used, for example, when powering the robot.

The passive wheels are fixed to the body with velcro stripes. In the experiments described in this paper, the wheels were fixed to the robot only for serpentine locomotion (not for swimming). We are currently investigating how the transition from serpentine locomotion to swimming (and vice-versa) could be realized; several options are considered (e.g. wheels, skates, etc.).

### C. Electrical description

Five wires pass all along the robot, one of which is currently unused. Two wires are used by the $I^2C$ bus, the third is the ground (common to the power and the bus), and the fourth is the optional external power source, mainly used to charge the batteries.

Inside each element are two double-sided printed circuits. The main elements of the first one are a power switch (for switching between battery and external power), a step-up converter to generate 5 V for the microcontroller when the circuit is powered by the 3.6 V Li-Ion battery, and a battery charger.

The core of the second circuit is a PIC microcontroller, containing a DC motor controller code (PID) developed at the Autonomous Systems Laboratory (ASL) of the EPFL. The PIC drives a low voltage H-bridge connected to the 0.75 W DC motor, and receives inputs from a quadrature detector (which filters and decodes the signals coming from the incremental encoder on the motor) and from an operational amplifier, which allows a measure of the voltage drop on a 0.2 $\Omega$ resistor inserted between the H-bridge and the motor, thus allowing an indirect measurement of the motor's torque. The parameters of the motor controller (i.e. current position, setpoint, PID factors, etc.) can be read and written over the $I^2C$ bus (each PIC has its own address programmed in the internal EEPROM memory).

The $I^2C$ bus is currently connected to an external PC using a RS-232 $\leftrightarrow$ $I^2C$ interface. A bidirectional wireless link is currently under development, and on-board trajectory generation is planned.

For more details concerning the robot, see [15].

## IV. Locomotion characterization

In order to test the locomotor abilities of the robot, we tested it using a range of different sine-based undulations. The parameters characterizing the sinusoidal crawling or swimming gaits are the amplitude $A$, the frequency $\nu$ and the phase lag $\Delta\phi$.

The setpoint sent to the robot at time $t$ for the $i^{\text{th}}$ joint is calculated using the following equation:

$$\theta_i(t) = A \cdot \sin(2\pi \cdot \nu \cdot t + 2\pi \cdot \Delta\phi \cdot (i-1)) \qquad (1)$$

For more clarity, we used the total phase lag between head and tail $N \cdot \Delta\phi$ (i.e. the inverse of the wavelength) as a measure of the phase lag, where $N$ is the number of active joints in the robot, so that our measure of phase is independent of the number of joints. An undulation with $N \cdot \Delta\phi = 1.0$ corresponds to an undulation in which the body makes a complete wave.

The speed of locomotion is measured with the following procedures. For crawling, the robot is moved to its start position (sending the $\theta_i$ setpoints for $t = 0$), then placed on

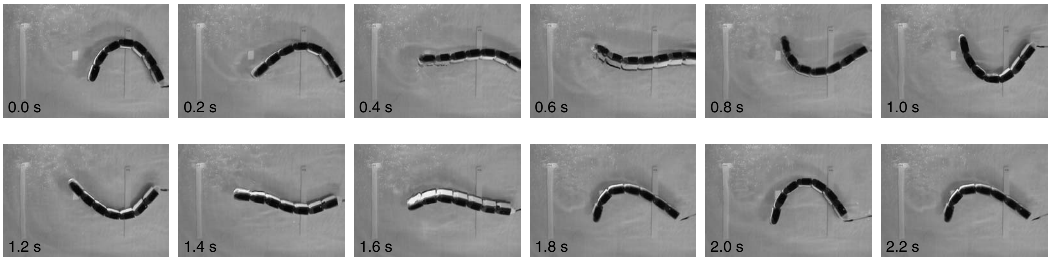


Fig. 2. The robot swimming in water with the optimal parameters ($A$ = 40°, $N \cdot \Delta\phi = 0.25$ and $\nu$ = 0.5 Hz).

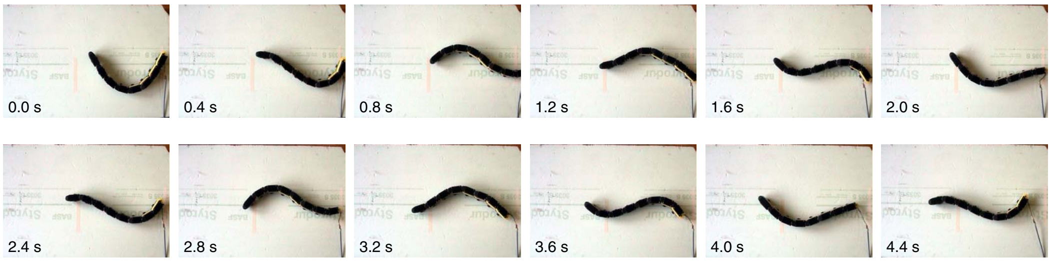


Fig. 3. The robot crawling on ground ($A$ = 30°, $N \cdot \Delta\phi = 0.5$ and $\nu$ = 0.5 Hz).[1]

a Styrodur® surface. The setpoints for the locomotion are then sent to the robot after starting the stopwatch (which is integrated in the control program). The locomotion is automatically stopped after 60 s, or manually if the limit of the surface is being reached. The covered distance is manually measured with a reel meter.

For swimming, the robot is placed in the water in a reset position (i.e. with all setpoints at 0°). The setpoints are then sent to the robot. If the robot does not cross a first line at 30 cm in less than 40 seconds (i.e. if it doesn't reach a mean speed of $7.5 \cdot 10^{-3}$ m/s during the first 40 s), the speed is considered as too low and set to null. If the measure is not null, a stopwatch is started when the robot's tail crosses the first line. A second line is placed at 50 cm from the first one: the stopwatch is stopped when the tail crosses it.

These procedures ensure that we measure the steady-state velocity during locomotion (for instance, we do not take into account the acceleration phase during swimming). Using this methodology, we systematically tested velocities in water and on ground with all possible combinations of parameters within the following ranges: $A \in [10; 15; 20; 25; 30; 35; 40]$ (°), $N \cdot \Delta\phi \in [0.25; 0.5; 0.75; 1.0; 1.25; 1.5]$, and $\nu \in [0.25; 0.5]$ (Hz). The maxima of these ranges corresponds to hardware limits of our robot.

## V. Results

### A. Swimming

Swimming results are presented in Figures 4(a) and 5(a) for $\nu = 0.25$ Hz and $\nu = 0.5$ Hz. The results for $\nu = 0.75$ Hz are not included, because we found out that the torque requirements for undulations with large amplitudes exceed our motor capabilities (i.e. actual trajectories become significantly different from the desired trajectories, exhibiting limited amplitudes and triangular waveforms). Snapshots of a swimming experience are shown in Figure 2.

The highest speed, $4.54 \cdot 10^{-2}$ m/s, is achieved with $\nu = 0.5$ Hz, $A = 40°$ and $N \cdot \Delta\phi = 0.25$. This corresponds to approximately 0.1 body lengths per second. The total phase lag between head and tail of $N \cdot \Delta\phi = 0.25$, which corresponds to a wavelength of 4 times the bodylength. It means that the body makes a travelling C-shape, rather than an S-shape.

Within the explored parameter space, the speed of swimming increases with the amplitude and with the frequency. It also increases inversely proportionally to the phase lag. Preliminary measures with values of $N \cdot \Delta\phi < 0.25$ show that the speed does not increase any further.

It should be noted that the region in parameter space corresponding to fast swimming is very small. It is indeed a peaked optimum, and large areas in the parameter space produce only very slow swimming. For instance, all measures for $N \cdot \Delta\phi \geq 1$ are below the $7.5 \cdot 10^{-3}$ m/s threshold during the first 40 seconds of swimming, and therefore considered null. These data therefore suggest that it is very important to find the right undulation for a given snake robot in order to obtain fast and efficient swimming.

### B. Crawling

The results obtained for crawling (also called serpentine, or lateral undulatory locomotion) are plotted in Figures 4(b) and 5(b). Snapshots of a crawling experience are shown in Figure 3.

The maximum locomotion speed of $3.33 \cdot 10^{-2}$ m/s is obtained with $\nu = 0.25$ Hz, $A = 40°$ and $N \cdot \Delta\phi = 0.5$. This corresponds to approximately 0.07 body lengths per second. It is approximately 30% slower than the fastest swimming gait.

[1] The parameters used in these snapshots are not optimal but only near the optimum. The snapshots with the optimal gait have not been realized for technical reasons.

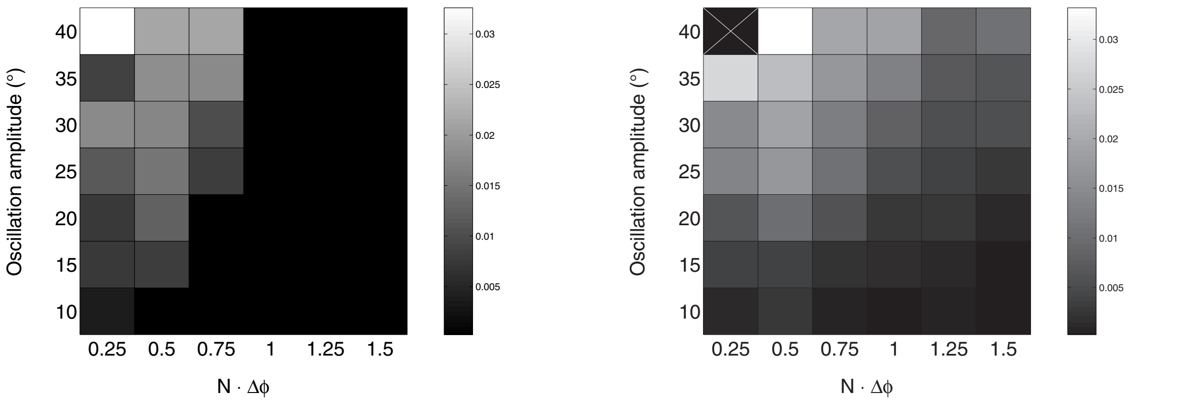


(a) Swimming (b) Crawling

Fig. 4. Locomotion characterization at $\nu = 0.25$ Hz. The cross in the second plot corresponds to parameters that cause the robot to fall over.

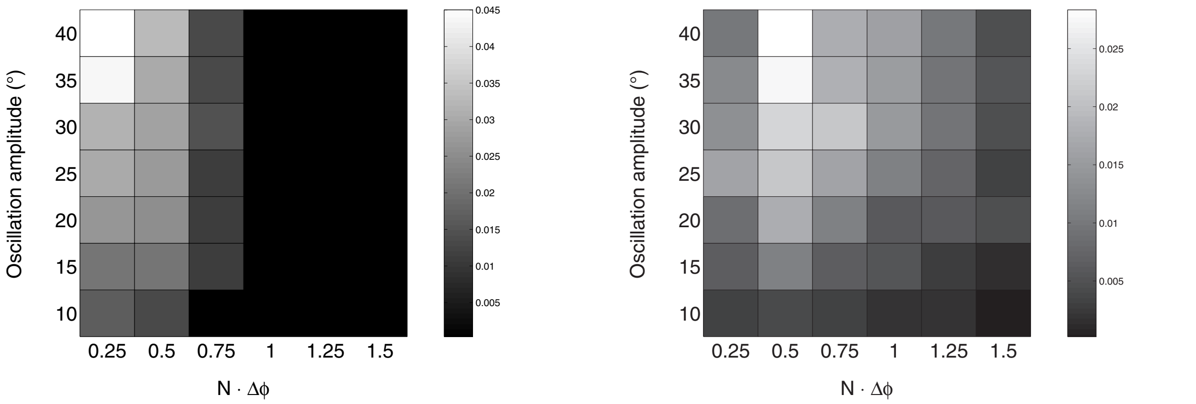


(a) Swimming (b) Crawling

Fig. 5. Locomotion characterization at $\nu = 0.5$ Hz

Similarly to swimming, the speed of crawling increases with the amplitude within the parameter space that we explored. Unlike swimming, the frequency did not significantly influence the speed of locomotion, and the fastest crawling is obtained with the lowest frequency $\nu = 0.25$ Hz. The optimal total phase lag $N \cdot \Delta\phi = 0.5$ is twice the one for swimming. A significant difference with swimming is the fact that the optimal region is larger and less peaked than for swimming. Fast crawling seems therefore less sensitive to the parameters of the undulation.

## VI. Discussion

We presented experiments for characterizing how the speed of locomotion depends on the frequency, amplitude, and phase lag of undulatory gaits, both in water and on ground. There have been relatively few studies of this kind, and to the best of our knowledge, none with a comparison of the two modes of locomotion. Analysis of the speed of serpentine locomotion can be found in [16], [17]. The results presented in these papers, however, cannot be compared directly to ours, as their authors were varying different parameters of a serpenoid curve ($\alpha_0$, corresponding to our amplitude parameter $A$, and $K_n$ in [16]) and of the environment (the friction coefficients $\mu_{t,n}$ in [16] and the inclination of the slope in [17]). The used serpenoid curve is also slightly different from our sinus wave, and cannot thus be directly compared.

Our results show that the speed of locomotion depends smoothly on the frequency, amplitude, and phase lag. For a given frequency, the optimal regions are unique (i.e. without multiple optimums). Interestingly the optimal regions are larger for crawling than for swimming, which means that the speed of crawling is less sensitive to the choice of undulations. These results can help designing optimization algorithms for adapting a locomotion controller to a specific environment. Further experiments should however be carried out with different ground surfaces in order to determine how friction properties affect the crawling speeds.

An interesting outcome of our experiments is that the fastest gaits are obtained with total phase lags between head and tail which are smaller than one, especially in water. This corresponds to wavelengths that are larger than one body length, in other words, to C-shaped undulations rather than S-shaped undulations. This is unlike the swimming of the lamprey or the eel, for instance, which tend to maintain a total phase lag of one. The fact that our robot has only 7 degrees of freedom might have played a role in making swimming with larger phase lags less fast (fewer degrees of freedom indeed mean that the undulation is less smooth). Another explanation could be the fact that lamprey and eel swim at higher frequencies (usually above 3 Hz), and that the fastest swimming gaits are obtained with larger phase lags at those frequencies.

Similarly to studies of amphibious snakes [18], we find that the velocities are higher during swimming than during serpentine locomotion (for the same frequencies in our experiments). Swimming is reported to be approximately twice as fast as crawling for most studied species in [18] (however without information on the characteristics of the undulation).

It should be noted that we currently explored only a subset of all possible gaits, as only sinus waves have been used. We plan to test in the future other signal shapes (e.g. with increasing amplitudes along the body, like those observed in lampreys).

## VII. Future work

Our experiments show several limitations of the current prototype of our robot. Several improvements can be made to develop the next prototype. The speed and power of the motors have to be increased. Simulations (not presented in this paper) show, for instance, that the speed of swimming increases approximately linearly with the frequency up to a saturation limit, which is really higher than the current maximum speed of the motors. The power of the motors has to be increased accordingly to produce the necessary torques and compensate the inertia and internal friction of the mechanics. The robot should then have the possibility to be completely autonomous. The current version is independent from the energetic point of view, but not for the control; all the information required to control the robot is currently sent from an external source (currently a PC), using the $I^2C$ bus. In order to achieve real autonomy, we plan to integrate a microcontroller or microprocessor in the head. A small bidirectional wireless link with low energy consumption is also under development, to get rid of the cable we currently need to use. As an additional improvement, it is also possible to consider the addition of more degrees of freedom: current elements have only one degree of freedom along the vertical axis, so that crossing obstacles, even small sized ones, could be a major problem. As the practical goal of the project is a robot that can be used for inspection tasks in difficult environments, more degrees of freedom (either passive or active) are desirable.

## VIII. Conclusion

This paper presented AmphiBot I, an amphibious snake-like robot capable of swimming and serpentine locomotion. The design considerations behind the robot's hardware were presented. The main contribution of this article is a detailed characterization of how the frequencies, amplitudes, and phase lags of undulatory gaits affect the speed of locomotion, both in water and on ground. To the best of our knowledge this study is the first of its kind. It should provide useful information for the design of the structure and controller of future amphibious snake robots.

## Acknowledgments

We gratefully acknowledge the support from Francesco Mondada and the Autonomous Systems Laboratory (ASL) at the EPFL, for their PD motor controller; from Daniel Burnier, for providing the RS-232 $\leftrightarrow$ $I^2C$ interface; and from Jérôme Braure for helping with the development of the simulation of the robot in Webots. This research is funded by a Young Professorship Award to Auke Ijspeert from the Swiss National Science Foundation.

## References

[1] A.J. Ijspeert. A connectionist central pattern generator for the aquatic and terrestrial gaits of a simulated salamander. *Biological Cybernetics*, 85(5):331–348, 2001.

[2] Y. Umetani and S. Hirose. Biomechanical study of active cord mechanism with tactile sensors. In *Proceedings of the 6th international symposium on industrial robots*, pages c1-1–c1-10, Nottingham, 1976.

[3] S. Hirose. *Biologically Inspired Robots (Snake-like Locomotor and Manipulator).* Oxford University Press, 1993.

[4] G.S. Chirikjian and J.W. Burdick. Design, implementation, and experiments with a thirty-degree-of-freedom 'hyper-redundant' robot. In *ISRAM 1992*, 1992.

[5] T. Lee, T. Ohm, and S. Hayati. A highly redundant robot system for inspection. In *Proceedings of the conference on intellingent robotics in the field, factory, service, and space (CIRFFSS '94)*, pages 142–149, Houston, Texas, 1994.

[6] G.S.P. Miller. *Neurotechnology for biomimetic robots*, chapter Snake robots for search and rescue. Bradford/MIT Press, Cambridge London, 2002.

[7] M. Saito, M. Fukaya, and T. Iwasaki. Serpentine locomotion with robotic snakes. *IEEE Control Systems Magazine*, 22:64–81, 2002.

[8] J. Conradt and P. Varshavskaya. Distributed central pattern generator control for a serpentine robot. In *ICANN 2003*, 2003.

[9] K. Dowling. *Limbless Locomotion: Learning to Crawl with a Snake Robot*. PhD thesis, Robotics Institute, Carnegie Mellon University, Pittsburgh, PA, December 1997.

[10] R. Worst. Robotic snakes. In *Third German Workshop on Artifical Life*, pages 113–126. Verlag Harri Deutsch, 1998.

[11] K.A. McIsaac and J.P. Ostrowski. A geometric approach to anguilliform locomotion: Simulation and experiments with an underwater eel-robot. In *ICRA 1999: Proceedings of 1999 IEEE International Conference on Robotics and Automation*, pages 2843–2848. IEEE, 1999.

[12] C. Wilbur, W. Vorus, Y. Cao, and S.N. Currie. *Neurotechnology for biomimetic robots*, chapter A Lamprey-Based Undulatory Vehicle. Bradford/MIT Press, Cambridge London, 2002.

[13] S. Hirose and E.F. Fukushima. Snakes and strings: New robotic components for rescue operations. In B. Siciliano and D. Paolo, editors, *Experimental Robotics VIII: Proceedings of the 8th International Symposium ISER02*, pages 48–63. Springer-Verlag, 2002.

[14] T. Takayama and S. Hirose. Amphibious 3D active cord mechanism "HELIX" with helical swimming motion. In *Proceedings of the 2002 IEEE/RSJ International Conference on Intelligent Robots and Systems*, pages 775–780. IEEE, 2002.

[15] A. Crespi, A. Badertscher, A. Guignard, and A.J. Ijspeert. Amphibot i: an amphibious snake-like robot. *Robotics and Autonomous Systems*. In press.

[16] S. Ma, H. Araya, and L. Li. Development of a creeping snake-robot. In *Proceedings of the 2001 IEEE International Symposium on Computational Intelligence in Robotics and Automation*, pages 77–82. IEEE, 2001.

[17] S. Ma, N. Tadokoro, B. Li, and K. Inoue. Analysis of creeping locomotion of a snake robot on a slope. In *ICRA 2003: Proceedings of the 2003 IEEE International Conference on Robotics and Automation*, pages 2073–2078. IEEE, 2003.

[18] R. Shine, H.G. Cogger, R.R. Reed, S. Shetty, and X. Bonnet. Aquatic and terrestrial locomotor speeds of amphibious sea-snakes (Serpentes, Laticaudae). *Journal of Zoology*, 259:261–268, 2003.